Megf10 regulates the progression of the satellite cell myogenic program

Chet E. Holterman,[1,2] Fabien Le Grand,[2] Shihuan Kuang,[2] Patrick Seale,[3] and Michael A. Rudnicki[1,2,3]

[1]Department of Cellular and Molecular Medicine, University of Ottawa, Ottawa, Canada K1N 6N5
[2]The Sprott Center for Stem Cell Research, Ottawa Health Research Institute Regenerative Medicine Program, Ottawa, Canada K1H 8L6
[3]Department of Biology, McMaster University, Hamilton, Canada L8S 4K1

We identify here the multiple epidermal growth factor repeat transmembrane protein Megf10 as a quiescent satellite cell marker that is also expressed in skeletal myoblasts but not in differentiated myofibers. Retroviral expression of Megf10 in myoblasts results in enhanced proliferation and inhibited differentiation. Infected myoblasts that fail to differentiate undergo cell cycle arrest and can reenter the cell cycle upon serum restimulation. Moreover, experimental modulations of Megf10 alter the expression levels of Pax7 and the myogenic regulatory factors. In contrast, *Megf10* silencing in activated satellite cells on individual fibers or in cultured myoblasts results in a dramatic reduction in the cell number, caused by *myogenin* activation and precocious differentiation as well as a depletion of the self-renewing $Pax7^{+}/MyoD^{-}$ population. Additionally, *Megf10* silencing in $MyoD^{-/-}$ myoblasts results in down-regulation of Notch signaling components. We conclude that Megf10 represents a novel transmembrane protein that impinges on Notch signaling to regulate the satellite cell population balance between proliferation and differentiation.

Introduction

Identified by their unique position between the myofiber basal lamina and the overlying plasmalemma (Mauro, 1961; Bischoff, 1994), satellite cells have been the object of intensive study for the past several decades, owing to their central role in muscle repair. More recently, several markers, including transcription factors such as Pax7 and Foxk1/myocite nuclear factor and cell surface markers such as c-Met/scatter factor receptor, syndecan 3 and 4, and M-cadherin, have been shown to be expressed in quiescent satellite cells, which allows for easy immunological identification (Holterman and Rudnicki, 2005).

In normal resting adult skeletal muscle, satellite cells are found in a mitotically quiescent state but can be induced to enter the cell cycle by weight bearing, trauma, and specific disease states. Activated satellite cells give rise to a transient amplifying population of myogenic precursor cells that undergo several rounds of division before undergoing terminal differentiation and fusing with existing fibers or forming new multinucleated fibers (Charge and Rudnicki, 2004). Furthermore, satellite cells also possess the ability to undergo self-renewal, effectively repopulating the quiescent satellite cell compartment after activation (Zammit et al., 2004; Collins et al., 2005; Kuang et al., 2007). Based on several observations, including different proliferative capacities and variability in expression of specific markers such as CD34 and *Myf-5*, it has been suggested that satellite cells are a heterogeneous population (Schultz, 1996; Beauchamp et al., 2000). Recent work from our laboratory has indicated that these differences likely reflect the hierarchical relationship between stem cells and committed cells within the satellite cell compartment (Kuang et al., 2007).

Despite our ability to identify quiescent satellite cells in resting muscle, much remains to be determined regarding the molecular mechanisms governing the activation of satellite cells and repopulation of the quiescent pool. Studies demonstrate that hepatocyte growth factor/scatter factor, the ligand for the c-Met receptor tyrosine kinase, plays a role in satellite cell activation or proliferation (Jennische et al., 1993; Tatsumi et al., 1998, 2001, 2006). In addition, research suggests that nitric oxide plays a functional role in the release of hepatocyte growth factor/scatter factor from the extracellular matrix, which implicates nitric oxide in satellite cell activation (Anderson, 2000; Tatsumi et al., 2002, 2006; Wozniak and Anderson, 2007).

Recent work also demonstrates that Notch activation occurs simultaneously with satellite cell activation both in vitro and in vivo (Conboy and Rando, 2002). The activation of the

C.E. Holterman and F. Le Grand contributed equally to this paper.

Correspondence to Michael A. Rudnicki: mrudnicki@ohri.ca

Abbreviations used in this paper: DIG, digoxigenin; EDL, extensor digitorum longus; GAPDH, glyceraldehyde 3–phosphate dehydrogenase; MyHC, myosin heavy chain; RDA, representational difference analysis; shRNA, short hairpin RNA.

The Journal of Cell Biology, Vol. 179, No. 5, December 3, 2007 911–922
http://www.jcb.org/cgi/doi/10.1083/jcb.200709083

Notch signaling pathway corresponds with the entry of satellite cells into a highly proliferative phase, during which the myogenic regulatory factors *MyoD* and *Myf5* are activated (Cornelison and Wold, 1997). Furthermore, it has been demonstrated that inhibition of Notch signaling by the Notch inhibitor Numb results in the terminal differentiation of committed myogenic precursors (Conboy and Rando, 2002). Downstream effectors of Notch signaling such as RBP-J and Stra13 appear to play crucial roles in mediating Notch signaling in activated satellite cells (Sun et al., 2007; Vasyutina et al., 2007). Differential expression of components of the Notch signaling pathway has been demonstrated within the satellite cell compartment, supporting the notion that heterogeneity within this population reflects its hierarchical nature (Conboy et al., 2003, 2005; Kuang et al., 2007).

In this study we characterize Megf10, initially cloned in representational difference analysis (RDA) studies designed to identify genes that functioned in the activation and maintenance of the satellite cell compartment (Seale et al., 2004). Megf10 is the mouse homologue of human MEGF10, a multiple EGF repeat–containing protein that localizes to the plasma membrane (Hamon et al., 2006; Suzuki and Nakayama, 2007). We reveal a novel role for Megf10 in regulating the proliferation and differentiation of mouse skeletal muscle satellite cells. Our experiments indicate that Megf10 activates Notch signaling to suppress progression of the differentiation program of sublaminar satellite cells and sustain their self-renewal.

Results

Isolation of full-length Megf10

The RDA clone MDp67 (Seale et al., 2004) was used as a probe to screen a λ-phage mouse skeletal muscle cDNA library for a full-length cDNA. Two positive plaques with identical overlapping sequences were isolated, revealing MDp67 to be the mouse homologue of human MEGF10 with >94% identity at the amino acid level. These two sequences are also similar to probable orthologues CED-1 (*Caenorhabditis elegans*) and Draper (*Drosophila melanogaster*; Zhou et al., 2001; Freeman et al., 2003).

Megf10 is expressed in adult skeletal muscle and proliferating myogenic precursors

To define the expression pattern of *Megf10* during the differentiation of wild-type and *MyoD*$^{-/-}$ primary myoblasts we performed quantitative PCR. Our results demonstrate down-regulation of *Megf10* upon serum withdrawal in wild-type myoblasts. Proliferating myoblasts were found to express 6.4-fold ($P = 0.035$) more *Megf10* than terminally differentiated myotubes (Fig. 1 A). *MyoD*$^{-/-}$ myoblasts, which fail to undergo terminal differentiation after serum withdrawal, maintained *Megf10* expression throughout the times examined (Fig. 1 A). Furthermore, our results demonstrated a 1.4-fold ($P = 0.05$) higher expression of *Megf10* in *MyoD*$^{-/-}$ myoblasts as compared with wild-type myoblasts maintained under the same growth conditions, and a much more pronounced 8.2-fold ($P = 0.004$) difference in expression 5 d after serum withdrawal.

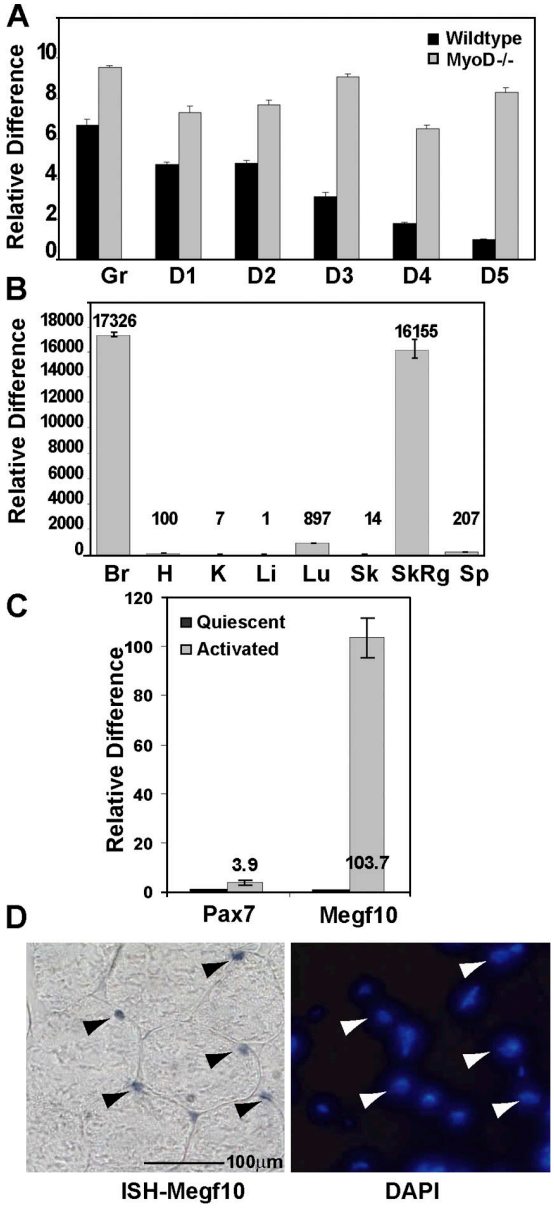

Figure 1. **Megf10 is expressed in proliferating myoblasts and resting adult skeletal muscle.** (A) Quantitative PCR was performed on samples from wild-type and MyoD$^{-/-}$ primary myoblasts cultured under growth (Gr) or differentiation (D1–D5) conditions. Samples were normalized to GAPDH and then to wild-type D5, which was set to a baseline expression of 1. Megf10 expression is down-regulated in wild-type myoblasts after serum withdrawal, whereas MyoD$^{-/-}$ myoblasts maintain Megf10 expression after serum withdrawal ($n = 3$). Error bars represent SEM. (B) Quantitative PCR demonstrating the relative expression of Megf10 in mouse tissues. All samples were normalized to GAPDH, and the lowest expressing tissue (liver) was set to a baseline expression of 1. High levels of Megf10 expression are detected in the brain and in regenerating (3 d after ctx injection) skeletal muscle ($n = 3$). Error bars represent SEM. Br, brain; H, heart; K, kidney; Li, liver; Lu, lung; Sk, skeletal muscle; SkRg, regenerating skeletal muscle; Sp, spleen. (C) Quantitative PCR showing the relative up-regulation of Pax7 and Megf10 gene expression levels during activation of satellite cells, RNA samples were extracted from freshly isolated FACS-sorted α7integrin^{+}, CD31/Sca1/CD45^{-} satellite cells (Quiescent) and in vitro–cultured myoblasts (Activated; $n = 3$). Error bars represent SEM. (D) In situ hybridization was performed with Megf10 antisense riboprobe on tibialis anterior muscle from 2-mo-old mice. Transcripts are located in fiber-associated cells in a position relative to satellite cells (arrowheads).

To determine if *Megf10* is expressed in a tissue-specific manner or is ubiquitously expressed throughout the organism, we performed quantitative PCR on RNA samples isolated from a variety of tissues. Very low levels of *Megf10* expression were detected in the majority of sample examined, including in resting skeletal muscle. However, high levels of *Megf10* expression were detected in the brain and in regenerating skeletal muscle 3 d after cardiotoxin injection, a pattern similar to that observed for human *MEGF10* (available at GenBank/EMBL/DDBJ under accession no. AB058676; http://www.kazusa.or.jp/huge/gfpage/KIAA1780/; Nagase et al., 2001; Fig. 1 B). To further address the issue of Megf10 up-regulation during regeneration, we FACS-sorted satellite cells from the limb muscles of 8-wk-old wild-type mice using the same protocol as described in Kuang et al. (2007). Purified cells are α7integrin$^+$, CD31$^-$/Sca1$^-$/CD45$^-$, and 94% positive for Pax7 expression. Quantitative PCR on cDNA prepared from freshly isolated satellite cells and satellite cells cultured in vitro for 3 d revealed that *Megf10* expression was up-regulated over 100-fold in activated satellite cells (Fig. 1 C).

To further verify the expression of *Megf10* in adult skeletal muscle, we performed in situ hybridizations on frozen sections from tibialis anterior muscles of 2-mo-old wild-type adult mice using a digoxigenin (DIG)-labeled antisense probe to *Megf10*. The results clearly demonstrated *Megf10* expression in cells located along the periphery of muscle fibers, which is consistent with expression in satellite cells (Fig. 1 D). Expression was detected in 5–7% of cells within resting muscle. These results verify that *Megf10* is expressed in resting adult skeletal muscle in a position and relative abundance consistent with quiescent satellite cells.

Megf10 is expressed in quiescent and activated satellite cells

To analyze expression of Megf10 protein in satellite cells, we generated rabbit polyclonal antisera that recognized the carboxy-terminal 290 aa of Megf10. Frozen sections of tibialis anterior muscle from 2-mo-old mice were costained with antibodies reactive to Megf10 and Syndecan-4 (Syn4), a known marker of quiescent satellite cells (Cornelison et al., 2001). Approximately 80% (147/185) of cells in a sublaminar satellite position that expressed Syn4 also expressed detectable levels of Megf10 (Fig. 2 A).

Individual myofibers were isolated together with their associated satellite cells, immediately fixed, and immunostained for Megf10, Pax7, and M-cadherin or Syn4. Approximately 80% (193/245) of Pax7- and M-cadherin–expressing quiescent satellite cells also expressed Megf10 (Fig. 2 B). Importantly, Megf10 was only expressed in cells that expressed Pax7 and was never detected in cells that did not express Pax7, verifying that Megf10 expression is restricted to quiescent satellite cells in resting adult skeletal muscle.

To investigate the pattern of Megf10 expression during myogenic activation, myofibers were cultured for 2 to 3 d in suspension, fixed and stained with a mix of antibody against Pax7, MyoD, and myogenin, which altogether marks the entire activated satellite cell population, and counterstained with Megf10. Virtually all (99.5%, 1,050/1,056) activated satellite cells stained positive for Megf10 (Fig. 2 D).

Megf10 was originally cloned from *MyoD*$^{-/-}$ primary myoblasts that express higher levels of Megf10 and Myf5 than wild-type myoblasts (Fig. 1 B). Therefore, to determine whether Megf10 expression is associated with Myf5 expression in satellite cells, we stained individual myofibers, freshly isolated from previously characterized *Myf5-Cre*ROSA-YFP* mice, for expression of YFP, Pax7, and Megf10 (Kuang et al., 2007). Interestingly Megf10 expression was detectable in 71% (135/189) of Pax7$^+$/YFP$^+$ committed progenitor cells but was not (0/11) observed in Pax7$^+$/YFP$^-$ satellite stem cells (Fig. 2 C). When fibers were maintained in culture for 3 d before fixing and staining, all Pax7-expressing activated satellite cells expressed Megf10, including YFP$^-$ cells (Fig. 2 E). Collectively these data suggest that although Megf10 may be correlated with Myf5 expression in a subset of satellite cells, Myf5 expression is not absolutely required for Megf10 expression.

Megf10 represses myogenic differentiation

To explore the biological function of Megf10 in myogenic cells, we infected 10T1/2 fibroblasts, primary myoblasts, and C_2C_{12} myoblasts with a retrovirus designed to express a full-length HA-tagged Megf10. Notably, we were unable to obtain viable primary myoblasts that overexpressed Megf10 after retroviral infection. In contrast, C_2C_{12} myoblasts and 10T1/2 fibroblasts overexpressing Megf10 were readily obtained. To verify the appropriate localization of retroviral-expressed Megf10, we performed immunocytochemistry (Fig. 3 B) and cellular fractionation on protein isolated from the cytoplasmic, plasma membrane, nuclear membrane, and nuclear compartments (Fig. 3 A). Western analysis of the fractions demonstrated that retrovirally expressed Megf10 localized to the plasma membrane, as well as to the cytoplasm of infected cells (Fig. 3 A). These results are consistent with recent publications demonstrating plasma membrane localization of MEGF10 (Hamon et al., 2006; Suzuki and Nakayama, 2007).

C_2C_{12} myoblasts overexpressing Megf10 were found to proliferate at a higher rate than empty vector controls, with a calculated 2.5-h decrease in their doubling time ($P = 0.012$; Fig. 3 C). TUNEL assays failed to demonstrate a significant change in the rate of apoptosis between Megf10-overexpressing cells ($0.59 \pm 0.21\%$) and empty vector controls ($0.69 \pm 0.17\%$) or un-infected cells ($0.64 \pm 0.18\%$; $n = 3$; $P = 0.44$). Importantly, forced expression of Megf10 in 10T1/2 fibroblasts did not alter their growth rate (unpublished data), suggesting that the effect of Megf10 on cell cycle progression is muscle specific.

We observed that *Megf10* expression was markedly down-regulated during myoblast differentiation (Fig. 1 A). Therefore, we asked whether or not sustained expression of Megf10 after serum withdrawal would have an effect on terminal differentiation. Myoblasts overexpressing Megf10 showed a dramatic decrease in terminal differentiation, as determined by immunocytochemistry (Fig. 4 A), and expressed markedly lower levels of myosin heavy chains (MyHC) as determined by Western blotting (Fig. 4 B). After 5 d in low-serum conditions, >80% (1,613/1,930) of empty-vector control cells had fused to form

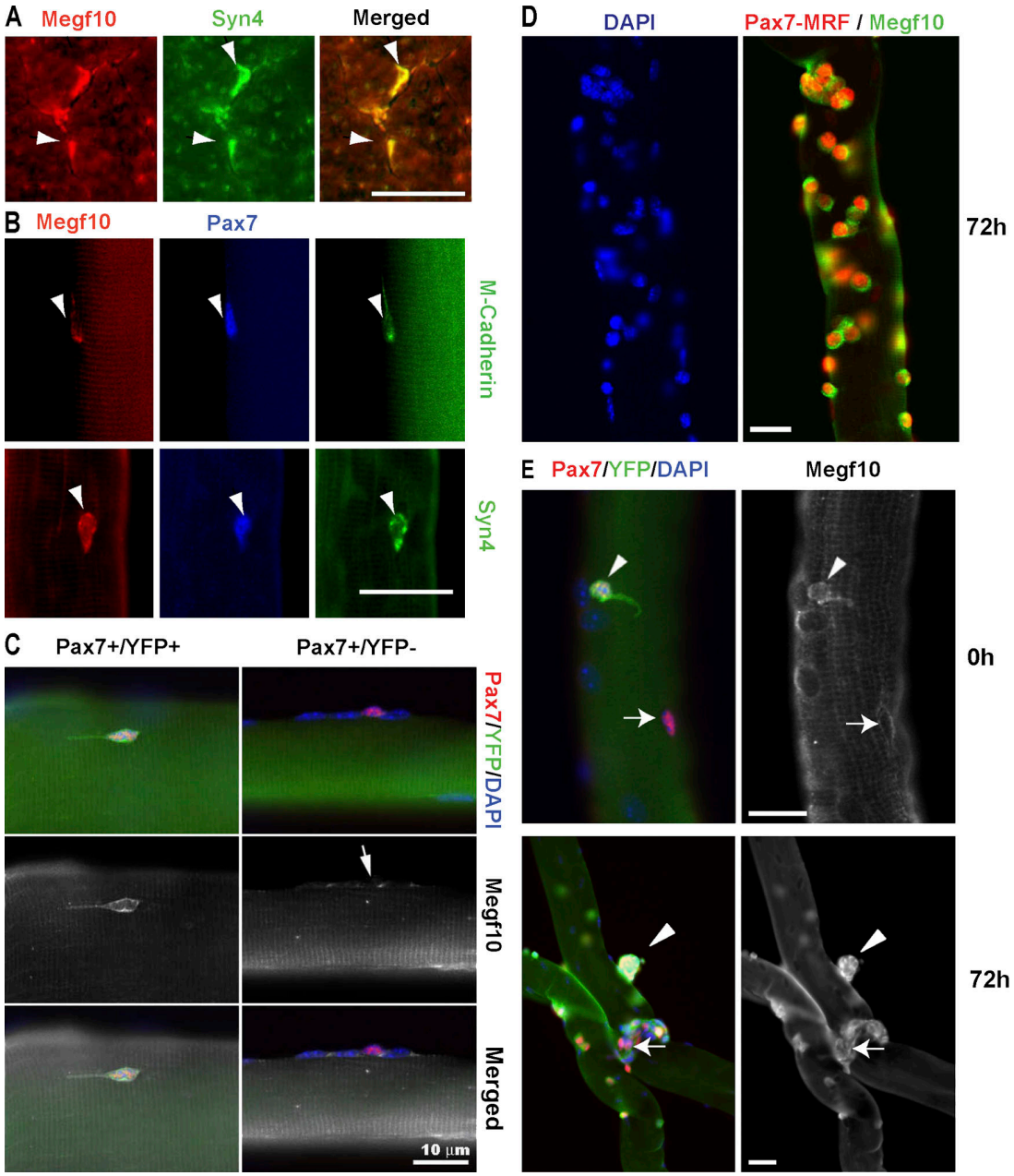

Figure 2. **Megf10 is expressed in quiescent and activated satellite cells.** (A) Immunohistochemistry on frozen sections of tibialis anterior muscles from 2-mo-old mice revealed that Megf10 was coexpressed with syndecan 4 in resting skeletal muscle. Arrowheads point to double-positive cells. Bar, 10 µm. (B) Individual myofibers isolated from the EDL muscle of adult mice were costained for Megf10, Pax7, and syndecan 4 or M-cadherin. Megf10 expression was limited to cells that also expressed Pax7 and syndecan 4 or M-cadherin (arrowheads), demonstrating that Megf10 expression is limited to quiescent satellite cells in resting skeletal muscle. Bar, 10 µm. (C) Individual fibers from the EDL muscle of Myf5-Cre*ROSA-YFP reporter mice were isolated, freshly fixed, and stained for YFP, Pax7, and Megf10 expression. Megf10 expression was detected in $Pax7^+/YFP^+$ quiescent satellite cells but never in $Pax7^+/YFP^-$ quiescent satellite cells. Arrow points to a $Pax7^+/YFP^-/Megf10^-$ satellite cell. (D) Myofibers were cultured for 3 d and stained for Pax7, MyoD, and myogenin in the same color to label all satellite cells. Counterstaining with the Megf10 antibody demonstrated that all (99.5%; $n > 1{,}000$) activated satellite cells express Megf10. Bar, 50 µm. (E) The presence of a $Pax7^+/YFP^+/Megf10^+$ progenitor cell (arrowhead) and a $Pax7^+/YFP^-/Megf10^-$ stem cell (arrow) on the same fiber after isolation. After 3 d in culture, both $Pax7^+/YFP^-$ (arrow) and $Pax7^+/YFP^+$ (arrowhead) proliferating cells express Megf10. Bars, 50 µm.

multinucleated MyHC-expressing cells (three or more nuclei/MyHC-positive body). In contrast, of the 15% (220/1,510) of cells overexpressing Megf10 that had undergone terminal differentiation, the majority (~50%) remained mononuclear (Fig. 4 C). Together these data strongly support the notion that ectopic Megf10 expression strongly inhibits myoblast differentiation and fusion (Fig. 4 C).

To further assess the terminal differentiation of these cells, we performed BrdU incorporation experiments. Under growth conditions, similar percentages of control and experimental cells incorporated BrdU (Fig. 5 A). 24 h after serum withdrawal, 25% (715/2,860) of control cells continued to incorporate BrdU, likely a result of a final round of cell division before terminal differentiation (Clegg et al., 1987). In contrast, only 5% (120/2,640) of

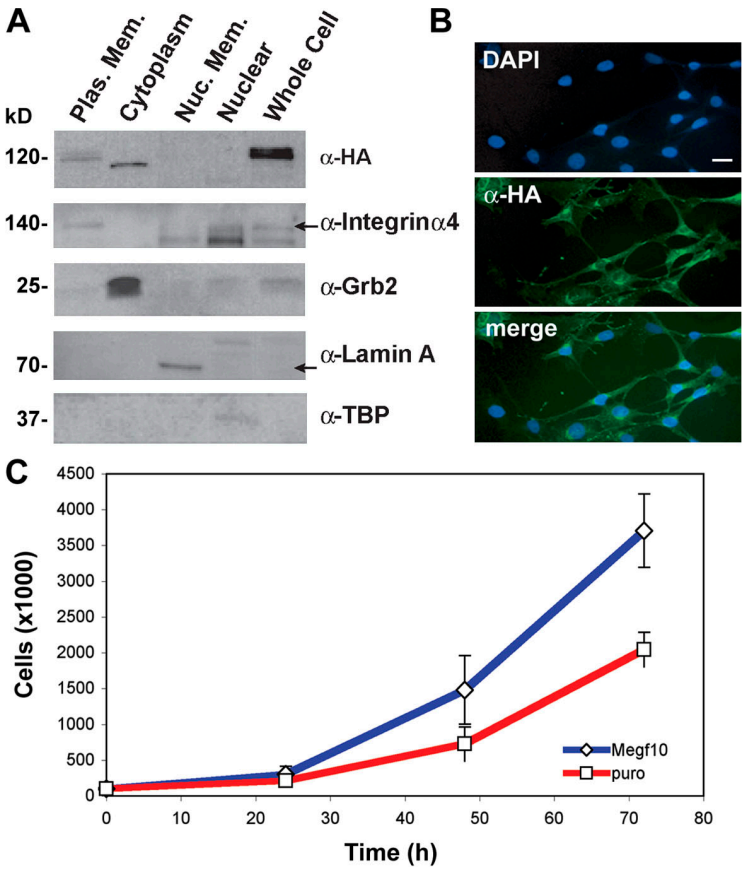

Figure 3. **Overexpression of Megf10 enhances proliferation of myogenic cells.** (A) C_2C_{12} myoblasts were infected with Megf10. Western blot with α-HA reveals Megf10 expression in the plasma membrane and cytoplasmic fractions. Fraction purity was examined by blotting for integrin α4 (plasma membrane), Grb2 (cytoplasm), Lamin A (nuclear membrane), and TBP (nuclear). Whole cell extract was used as a positive control. (B) Immunocytochemistry on infected cells demonstrated cytoplasmic and potential plasma membrane localization of Megf10 in infected cells but not controls. Bar, 10 μm. (C) C_2C_{12} cells infected with Megf10 or empty vector puro controls were counted at either 24, 48, or 72 h after plating (n = 9). Error bars represent SEM.

Megf10-overexpressing cells continued to incorporate BrdU at 24 h after serum withdrawal. 48 h after serum withdrawal, <5% of cells in both control and experimental populations incorporated BrdU, and this proportion did not change at later times. When myoblasts ectopically expressing Megf10 were exposed to low-serum conditions for 5 d and then restimulated with growth media for 24 h, 35% (632/1,355) of Megf10-overexpressing cells reentered the cell cycle as demonstrated by their ability to incorporate BrdU (Fig. 5 B). In contrast, <10% (136/1,420) of uninfected myocytes reentered the cell cycle after serum stimulation, most likely because of the presence of undifferentiated reserve cells present after induction of differentiation of C_2C_{12} cells (Yoshida et al., 1998). These data indicate that expression of Megf10 markedly inhibits myogenic differentiation under low-serum conditions. Moreover, infected myoblasts enter a reversible quiescent state rather than undergoing terminal differentiation.

Megf10 regulates key effectors of the myogenic program

To investigate the molecular basis for the change in growth kinetics and differentiation capacity of cells overexpressing Megf10, we examined the expression of key regulators of myogenic function. Strikingly, C_2C_{12} cells overexpressing Megf10 showed a dramatic down-regulation of MyoD and Pax7 proteins (Fig. 6 A). In addition, Western analysis revealed similarly decreased levels of Desmin and E-box–binding protein (unpublished data). In contrast, the level of Myf5 protein was increased. Examination of protein levels during differentiation revealed a failure of Megf10-overexpressing myoblasts to up-regulate myogenin (Fig. 6 A) and MyHC (Fig. 4 B) during differentiation.

Quantitative PCR analysis was performed to determine if the changes in Myf5, MyoD, and Pax7 protein levels reflected changes in the level of mRNA. Importantly, *Myf5* mRNA was up-regulated and *Pax7* mRNA was down-regulated to a similar degree as the changes in protein levels. In contrast, no significant change was detected in *MyoD* mRNA levels (Fig. 6 B). The results suggest a posttranscriptional down-regulation of MyoD protein levels in Megf10-expressing myoblasts.

Megf10 regulates the balance between proliferation and differentiation within the satellite cell compartment

Having demonstrated that Megf10 is expressed in all activated satellite cells and that forced expression of Megf10 inhibited differentiation of myogenic cells, we set out to determine whether Megf10 regulated the proliferative potential of activated satellite cells. Individual fibers were isolated from extensor digitorum longus (EDL) muscles of 8-wk-old mice and transfected after 24 h with Cy3-labeled siRNA against *Megf10*. siRNA-Cy3 incorporation by satellite cells was monitored 24 h after transfection, with an efficiency ranging from 51 to 79% (unpublished data). Fibers were maintained in culture for 72 h (48 h after transfection) and then stained for Pax7 and Megf10 expression. Loss of Megf10 immunostaining in the context of si-Megf10 transfections validated the efficiency of the knockdown (Fig. 7 A).

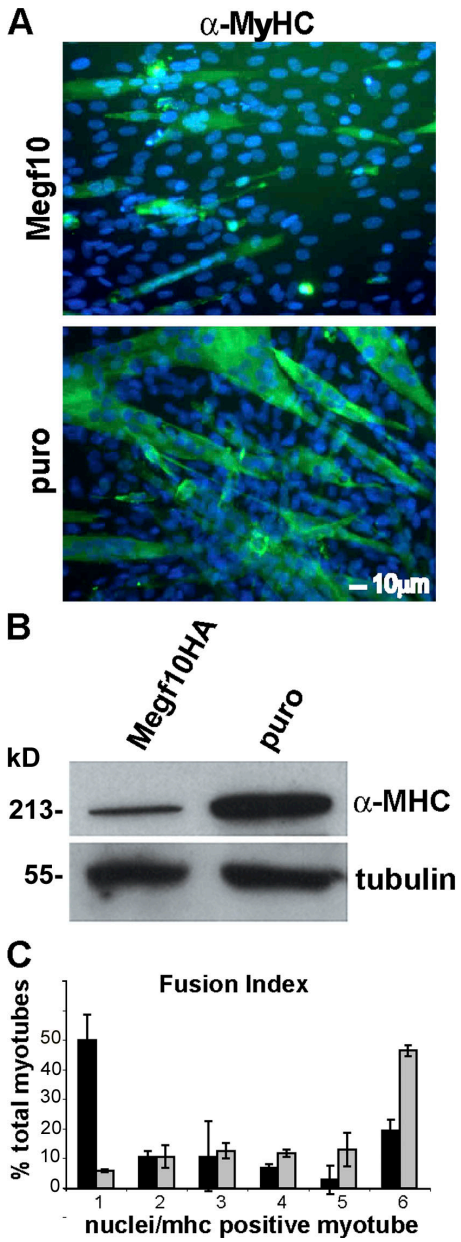

Figure 4. **Overexpression of Megf10 inhibits differentiation of myogenic cells.** (A) C_2C_{12} cells infected with Megf10 or empty vector puro controls were stained with α-MyHC. Cells overexpressing Megf10 displayed a dramatic decrease in differentiation as compared with controls. (B) Western blots reveal a dramatic decrease in MyHC expression at 5 d after serum withdrawal in cells overexpressing Megf10. (C) The number of nuclei per MyHC-positive body was examined and plotted to demonstrate that although <5% of MyHC-positive control cells remained mononuclear, 50% of MyHC-positive Megf10 cells failed to fuse to form multinucleated myotubes ($n = 3$). Error bars represent SEM.

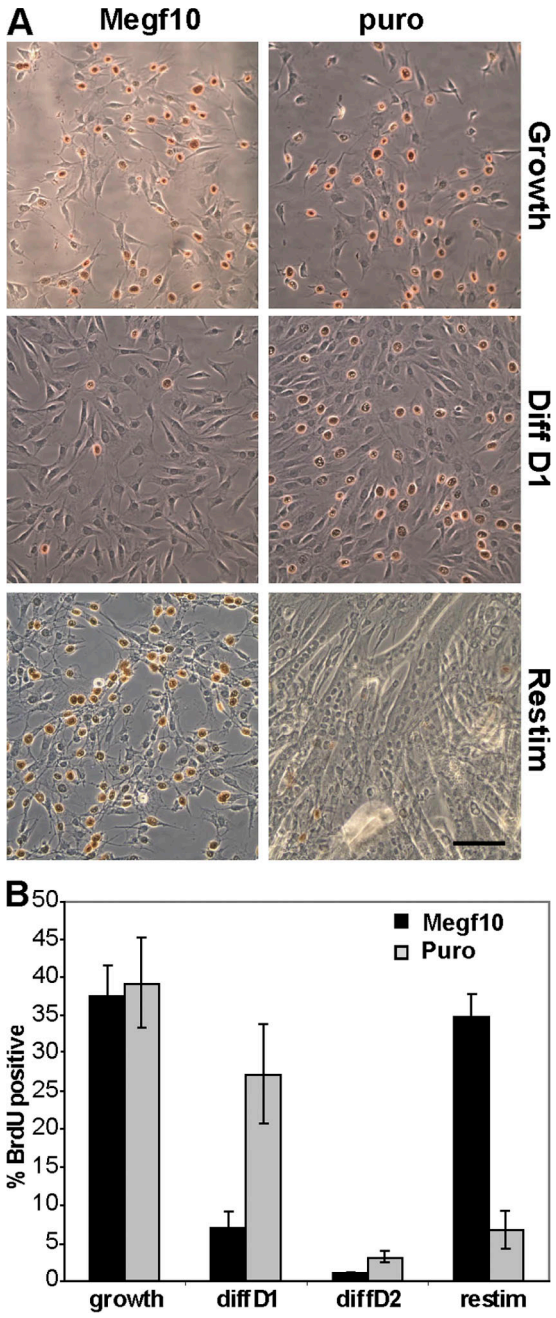

Figure 5. **Megf10 stimulates quiescence after serum withdrawal.** (A) C_2C_{12} myoblasts infected with Megf10 or empty vector puro control were maintained in growth media or differentiated for 1 to 5 d. Cells were stained for BrdU incorporation. Approximately 30% of cells incorporate BrdU under growth conditions. Within 24 h of serum withdrawal, only 8% of Megf10-expressing cells incorporate BrdU, indicating withdrawal from the cell cycle, whereas 25% of control cells incorporate BrdU. A large percentage of cells expressing Megf10 that were subjected to low serum were able to reenter the cell cycle, whereas the majority of control cells had terminally differentiated ($n = 3$). Bar, 100 μm. (B) Histogram demonstrating the number of cells that incorporated BrdU during a 30-min pulse after 120 h of differentiation and 24 h of restimulation ($n = 3$). Error bars represent SEM.

A 30% decrease ($n > 900$; $P = 0.05$) was observed in the mean number of activated satellite cells at the surface of isolated fibers (Fig. 7 B). Furthermore, a 62% ($n > 400$; $P = 0.009$) reduction was observed in the number of $Pax7^+/MyoD^-$ transient self-renewing cells (Fig. 7 C). Interestingly, the ratio of YFP^- stem cells to YFP^+ progenitor cells was unaltered ($n > 500$), suggesting a proportionate reduction in the number of cells in both populations (Fig. 7 D).

To determine if the reduction in the number of activated satellite cells was caused by premature differentiation, we analyzed Pax7 and myogenin protein expression in satellite cells on transfected fibers with si-scrambled and si-Megf10, at a time

before the cell-depleting effect of Megf10 knockdown takes place. We chose to fix and stain transfected fibers at 60 h in culture in vitro (36 h after transfection). At this time, activated satellite cells on fibers had gone through three doublings, and the mean number of activated cells per fiber was similar (si-scrambled: 51.25 ± 3.37 cells/fiber; si-Megf10: 50.24 ± 4.77 cells/fiber). As expected, we saw a major increase in the proportion of myogenin-expressing cells (3.15-fold increase; $n > 2{,}000$; $P = 0.0036$) after transfection of si-Megf10 as compared with si-scrambled. These results demonstrate that knockdown of Megf10 expression results in precocious differentiation of activated satellite cells (Fig. 8 A).

Transfection of primary myoblasts with siRNA against *Megf10* resulted in a 0.5-fold ($P < 10^{-5}$) decrease in *Megf10* expression and a corresponding 1.8-fold ($P < 10^{-3}$) increase in *myogenin* expression and a 2.5-fold ($P < 10^{-4}$) increase in *MyHC* expression, as determined by quantitative PCR, verifying increased differentiation upon *Megf10* silencing (Fig. 8 B). Interestingly, *Pax7*, *MyoD*, and *Myf5* expression were also down-regulated after siMegf10 transfection as a direct effect of *Megf10* knockdown forcing myogenic differentiation. These results further demonstrate the ability of Megf10 to regulate the proliferative potential of sublaminar satellite cells.

Megf10 impinges on the Notch signaling pathway

Recent work has indicated that the extracellular domain of JEDI, a Megf10 family member, is capable of modulating Notch signaling in a manner similar to members of the Jagged/Serrate/Delta family of Notch ligands (Krivtsov et al., 2007). We therefore examined expression levels of Notch signaling components after *Megf10* knockdown. Because the loss of *Megf10* expression leads to premature differentiation of primary myoblasts, we used *MyoD*$^{-/-}$ myoblasts, which cannot differentiate and more closely resemble satellite cells (Megeney et al., 1996; Sabourin et al., 1999; Seale et al., 2004). This allowed us to investigate the effects of Megf10 down-regulation on Notch signaling in a cellular context where the down-regulation of Notch signaling induced by differentiation cannot occur.

Cells were transiently transfected with a cocktail of three different plasmids containing unique short hairpin RNAs (shRNAs) against *Megf10*. Transfection efficiency was found to be 30% using β-galactosidase as a reporter. After transfection with the shRNA, *Megf10* expression was determined using quantitative real-time PCR. We detected a 0.56-fold ($P = 0.012$) reduction in overall levels of *Megf10* expression in cells transfected with *Megf10* shRNA as compared with a nonsilencing control (Fig. 8 C). We did not detect significant changes in the levels of *Pax7* or *Pax3* expression after *Megf10* knockdown; however, we did note a 1.5-fold ($P = 0.034$) increase in *Myf5* expression (Fig. 8 C). Notably, we observed down-regulation of Notch receptors *Notch 1* (0.56-fold; $P = 0.001$), *Notch 2* (0.64-fold; $P = 0.027$), and *Notch 3* (0.41-fold; $P = 0.018$), as well as down-regulation of Notch downstream effector *Hes 1* (0.52-fold; $P = 0.046$) after *Megf10* knockdown. No significant difference was observed in the expression of Notch ligands *Delta-like 1*, *Delta-like 4*, or *Jagged 1* (Fig. 6 D). These data support the notion that the extracellular domain of Megf10, similar to the corresponding domain of DSL proteins, activates Notch signaling. Collectively, these experiments suggest that Megf10 plays a key role in controlling the expression of key regulators of myogenic commitment and differentiation.

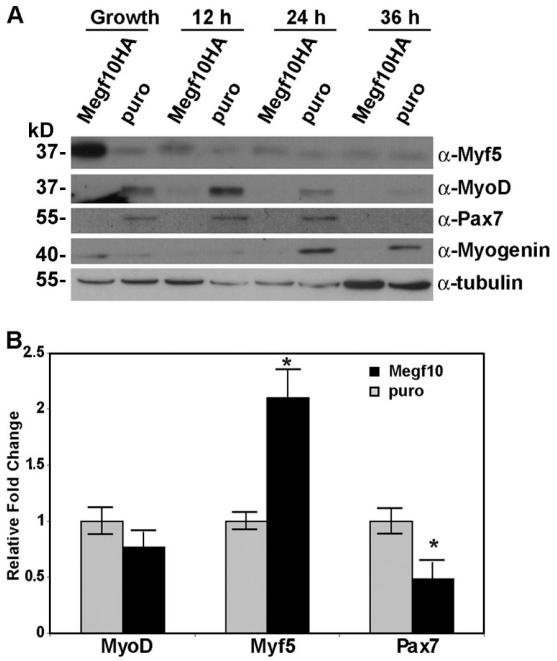

Figure 6. **Overexpression of Megf10 alters the levels of key myogenic proteins.** (A) Western blot of protein extracts from Megf10-overexpressing cells and empty vector puro controls. Myf5 levels are elevated in Megf10-overexpressing cells, whereas MyoD and Pax7 are down-regulated under growth conditions. Cells overexpressing Megf10 fail to up-regulate myogenin during differentiation. (B) Quantitative PCR analysis reveals that although Myf5 and Pax7 RNA levels are altered in Megf10-expressing cells, alterations in MyoD are occurring mainly at the protein level (*, $P < 0.02$). Transcript levels are normalized to GAPDH and control levels are set to 1 ($n = 3$). Error bars represent SEM.

Discussion

In recent years, several new markers of quiescent satellite cells have been identified, providing insight into the origins of these cells as well as the mechanisms by which they affect muscle regeneration. Using RDA, we have identified several potential satellite cell markers, including Megf10, a multiple EGF repeat–containing transmembrane protein (Seale et al., 2004). Although orthologues of Megf10 (CED-1 and Draper) have been previously identified and shown to function in engulfment of apoptotic cells during neurogenesis, a role for Megf10 in satellite cell function has not been previously described (Zhou et al., 2001; Freeman et al., 2003).

Megf10, although highly expressed in the brain, is also expressed in resting adult skeletal muscle, as determined by in situ hybridization, and its expression is up-regulated in response to injury as determined by quantitative PCR. Our immunohistochemical analysis on sections from tibialis anterior muscles and individual fibers isolated from EDL muscle clearly demonstrate that the expression of Megf10 is strictly limited to the majority

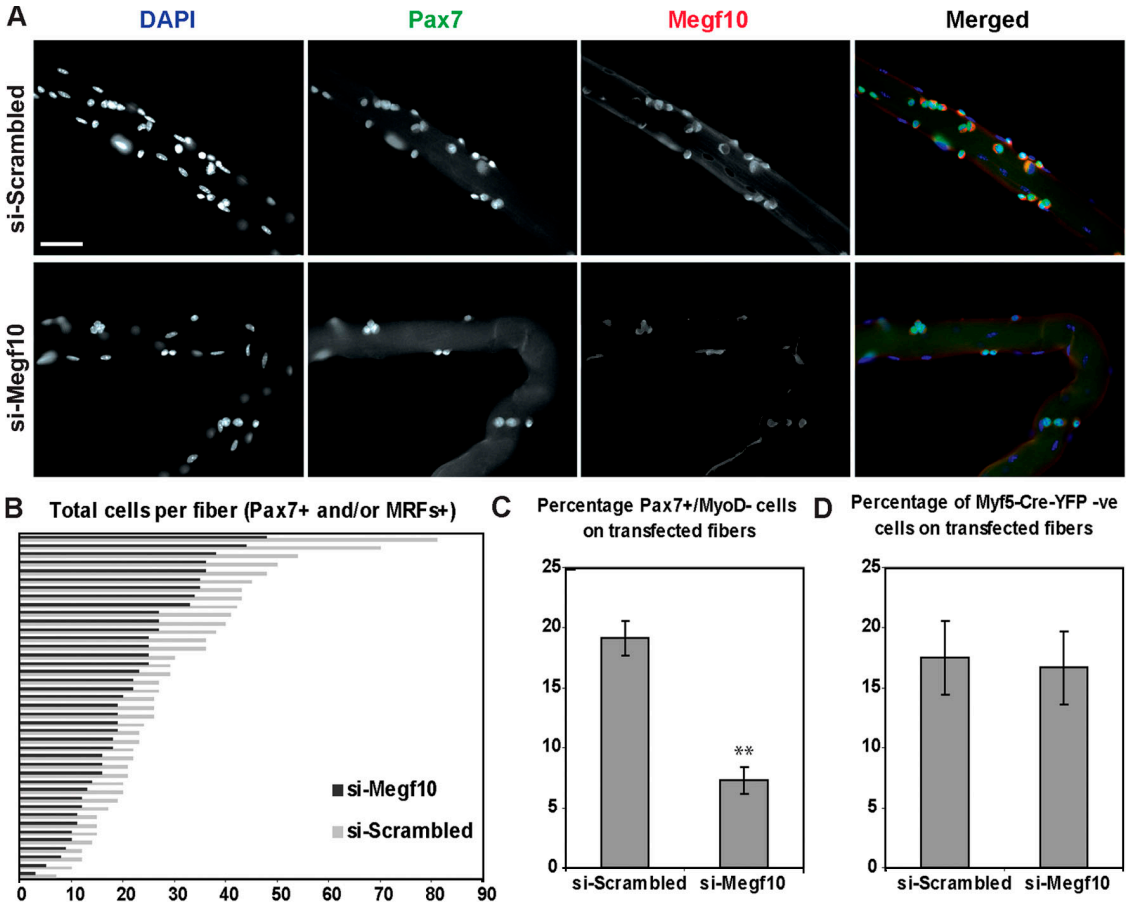

Figure 7. **Megf10 regulates satellite cell activation and proliferation.** (A) Individual fibers isolated from EDL muscles were transfected with Megf10 siRNA, cultured for 3 d, and stained for Pax7 and Megf10. siRNA knockdown induces a loss of Megf10 protein expression by the majority of the activated satellite cells ($n = 3$). Bar, 50 μm. (B) Histograms depicting individual counts of the total numbers of activated satellite cells (labeled with Pax7 and MyoD/myogenin) on fibers transfected with Megf10 siRNA. The mean number of myogenic cells per fiber is reduced by a mean of 30% as compared with scrambled siRNA controls ($n = 3$). (C) Knockdown of Megf10 dramatically reduces the number of self-renewing progenitors ($Pax7^+/MyoD^-$) from 19 to 7% and respectively increases the number of $Pax7^+/MyoD^+$ cells ($n = 3$; **, $P = 0.008$). Error bars represent SEM. (D) Although the number of activated progenitor cells is reduced, the overall ratio of stem cell (YFP^-) to progenitor cell (YFP^+) remains unchanged ($n = 3$). Error bars represent SEM.

of quiescent satellite cells in resting muscle. Although we only detected Megf10 in Myf5-Cre-$YFP^+/Pax7^+$ satellite cells, it is possible that Megf10 expression level in the quiescent Myf5-Cre-$YFP^-/Pax7^+$ satellite stem cell population is below detectable levels in our assays. Interestingly, we observed Megf10 expression in all satellite cells of individual fibers after activation, suggesting that all satellite cells up-regulate Megf10 upon activation. This is in agreement with our quantitative PCR analysis, which demonstrated significant up- regulation of *Megf10* in activated satellite cells.

Our results demonstrate that overexpression of Megf10 in myogenic cells in vitro results in enhanced proliferation. In wild-type myoblasts, *Megf10* expression is down-regulated during terminal differentiation. In cells modified to overexpress Megf10, expression is maintained after serum withdrawal and a dramatic inhibition of differentiation is observed. Importantly, cells overexpressing Megf10 exit the cell cycle within 24 h of serum withdrawal, as determined by BrdU incorporation, but maintain the ability to reenter the cell cycle through serum stimulation. These results suggest that maintained Megf10 expression allows cells to return to a quiescent state where they can respond to subsequent stimulation. Collectively, these data implicate Megf10 as being an important regulator of satellite cell function by suppressing the progression of the differentiation program of sublaminar satellite cells and thus enforcing self-renewal. It has recently been demonstrated that in the absence of Myf5, the transient activating population is dramatically compromised in adult skeletal muscle, and in response to injury, activated satellite cells undergo precocious differentiation in viable $Myf5^{-/-}$ mice (Ustanina et al., 2007). Thus, it would appear that although MyoD expression is required for the appropriate differentiation of activated satellite cells, Myf5 functions in the expansion and proliferation of these cells. Interestingly, cells overexpressing Megf10 express elevated levels of Myf5 and decreased levels of MyoD, much like $MyoD^{-/-}$ myoblasts, which show a propensity for proliferation and self-renewal rather than differentiation (Megeney et al., 1996; Sabourin et al., 1999). Although there is an increase in the level of *Myf5* RNA in these cells, it has not been determined if this is a direct effect of Megf10 overexpression stimulating *Myf5* transcription. Alternatively, repression of the *Myf5* locus may be relieved because of the absence of MyoD protein

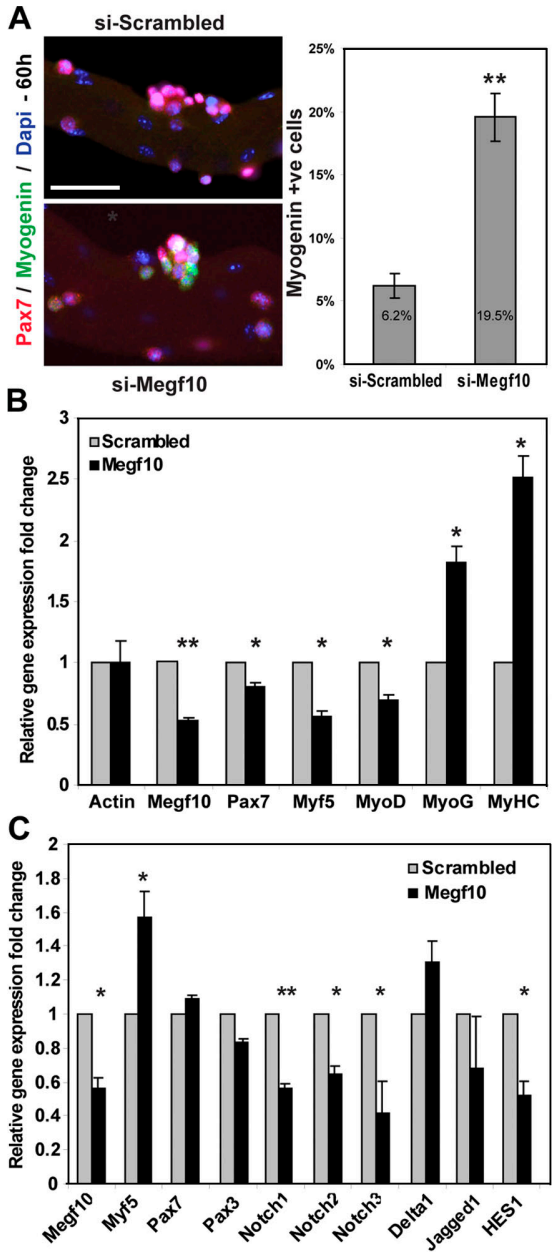

Figure 8. **Loss of Megf10 results in precocious differentiation.** (A) EDL fibers were transfected with Megf10 siRNA, cultured for 60 h, and stained for Pax7 and myogenin. Megf10 knockdown induces three times more cells to undergo precocious differentiation ($n = 3$; **, $P = 0.004$). Error bars represent SEM. Bar, 50 µm. (B) Quantitative PCR analysis demonstrates up-regulation of myogenin and MyHC and down-regulation of Pax7, MyoD, and Myf5 in wild-type primary myoblasts in which Megf10 has been knocked down ($n = 6$; *, $P < 0.05$; **, $P < 0.01$). Error bars represent SEM. (C) Quantitative PCR demonstrates down-regulation of components of the Notch signaling pathway after shRNA knockdown of Megf10 in MyoD$^{-/-}$ primary myoblasts ($n = 3$; *, $P < 0.05$; **, $P < 0.01$). Error bars represent SEM.

(Megeney et al., 1996). We believe the latter to be the case, as knockdown of *Megf10* expression in *MyoD*$^{-/-}$ myoblasts does not result in down-regulation of *Myf5*. In fact, *Myf5* transcript levels increase upon *Megf10* silencing. Interestingly, we have previously demonstrated that Myf5 levels are elevated at early time points after serum withdrawal in *MyoD*$^{-/-}$ myoblasts (Sabourin et al., 1999). Based on our results, one could speculate that Megf10 may suppress the progression of the differentiation program of sublaminar satellite cells by modulating Myf5 and MyoD expression.

The role of Megf10 in regulating the proliferative potential of the satellite cell compartment is further supported by our knockdown experiments in vitro and on individual fibers. In vitro, knockdown of Megf10 resulted in precocious differentiation of primary myoblasts maintained under growth conditions. Megf10 knockdown on individual fibers resulted in a pronounced decrease in the number of activated precursor cells because of precocious differentiation, as determined by a significant increase in the number of myogenin-expressing cells at 60 h, a time at which the number of cells per fiber (si-Megf10 vs. si-scrambled) is not significantly different. Megf10 knockdown also resulted in a concomitant reduction in the number of transient self-renewing cells per fiber after 72 h in culture. Furthermore, it is important to note that the overall proportion of Myf5-Cre-YFP^{-} stem cells to Myf5-Cre-YFP^{+} committed progenitor cells was unaltered, implying that loss of Megf10 expression results in precocious differentiation of both the stem and progenitor satellite cell populations. This is not unexpected, given that after activation all satellite cells express Megf10. These results imply a critical role for Megf10 in the appropriate self-renewal of the satellite cell compartment.

It has been well demonstrated that Notch signaling is a critical determinant in the progression of satellite cells toward myogenesis (Conboy and Rando, 2002). Satellite cell activation and proliferation is accompanied by an increase in expression of Notch receptors and Notch signaling, whereas terminal differentiation occurs after inhibition of Notch signaling (Conboy and Rando, 2002). All satellite cells express Notch-1 and satellite stem cells (YFP^{-}) express *Notch-3*, whereas the committed progenitor population (YFP^{+}) expresses the Notch ligand *Delta-like-1* (Kuang et al., 2007). Inhibition of Notch signaling results in a loss of the stem cell population and premature differentiation, suggesting that the Notch signaling pathway plays a crucial role in the self-renewal of satellite cells (Kuang et al., 2007).

Of interest is the potential interaction of Megf10 with the Notch signaling pathway. A recent publication demonstrates the ability of JEDI, a potential Megf10 family member, to regulate the Notch signaling pathway in a delta-like manner in hematopoietic cells (Krivtsov et al., 2007). Furthermore, it has been demonstrated that constitutive activation of Notch signaling in myoblasts results in enhanced proliferation and defective differentiation, a phenotype that is strikingly similar to that observed upon overexpression of Megf10 in myoblasts (Nofziger et al., 1999; Conboy and Rando, 2002).

Our results suggest that Megf10 regulates the proliferative capacity of myogenic cells, potentially via the Notch signaling pathway. With 30% transfection efficiency, we were able to reduce *Megf10* expression 0.56-fold overall in primary *MyoD*$^{-/-}$ myoblasts. This was accompanied by a reduction of Notch receptors' transcripts and down-regulation of *Hes1*, which can be directly linked to the precocious differentiation observed in wild-type myoblasts after Megf10 knockdown, a result reminiscent of a loss of Notch signaling. Up-regulation of *Myf5*

after *Megf10* silencing in *MyoD*$^{-/-}$ myoblasts, coupled with the observed decrease in *Notch* and *Hes1* transcript levels, suggests that down-regulation of *Megf10* allows cells to progress toward terminal differentiation. However, *Megf10* silencing did not rescue the differentiation deficit observed in *MyoD*$^{-/-}$ myoblasts (unpublished data), most likely because of the requirement for MyoD activity for subsequent differentiation.

It is curious that we only detected Megf10 expression in the committed progenitor population of quiescent satellite cells, which also express Delta-like-1, whereas it was up-regulated in all satellite cells after activation. Such heterogeneity within the quiescent satellite cell compartment has previously been described for other markers such as CD34 and *Myf5* as well as components of the Notch signaling pathway and may be indicative of the hierarchical nature of the satellite cell compartment (Beauchamp et al., 2000; Conboy et al., 2003, 2005; Kuang et al., 2007). Alternatively, the heterogeneity observed within the satellite cell compartment may reflect differences between naive satellite cells established during development and those that have been activated subsequent to their developmental establishment. Importantly, these concepts are not mutually exclusive.

Given the ability of Megf10 expression to alter growth and differentiation kinetics of myoblasts as well as the levels of key myogenic proteins, we hypothesize that Megf10 functions to maintain the satellite cell compartment. It does so by maintaining self-renewing cells' proliferation and by inhibiting their progression through the myogenic program and terminal differentiation. After activation of satellite cells, Megf10 may dictate whether a cell continues to proliferate, returns to a quiescent state, or enters the myogenic program to undergo terminal differentiation. This, we propose, is accomplished by modulating Notch signaling. Although the mechanism by which Megf10 expression is regulated remains to be elucidated, our findings demonstrate a novel and critical role for Megf10 in the regulation of satellite cell dynamics and maintenance.

Materials and methods

RNA isolation and real-time PCR
RNA was isolated using the RNeasy Miniprep kit (QIAGEN) and subjected to on column DNase digestion as per the manufacturer's instructions. RT-PCR of samples was performed using the Core PCR kit (PerkinElmer) using random hexamer primers. Real-time PCR was performed as previously described (Ishibashi et al., 2005). Transcript levels were normalized to glyceraldehyde 3–phosphate dehydrogenase (GAPDH) transcript levels. Relative fold change in expression was calculated using the ΔΔCT method (CT values < 30). Primer sequences for Pax7, Pax3, Megf10, Notch1, Notch2, Notch3, Delta1, Jagged, and Hes were as follows; Pax7, forward, CTGGATGAGGGCTCAGATGT; Pax7, reverse, GGTTAGCTCCTGCCTGCTTA; Pax3, forward, GCTGTCTGTGATCGGAACACT; Pax3, reverse, CTCCAGCTTGTTTCCTCCATC; Megf10, forward, ACTGGAGCCTTCTGTGAGGA; Megf10, reverse, ACACTGGCATTCTTGGGAAC; Notch1, forward, GGTCGCAACTGTGAGAGTGA; Notch1, reverse, TTGCTGGCACATTCATTGAT; Notch2, forward, GCAGGAGCAGGAGGTGATAG; Notch2, reverse, GCGTTTCTTGGACTCTCCAG; Notch3, forward, GTCCAGAGGCCAAGAGACTG; Notch3, reverse, CAGAAGGAGGCCAGCATAAG; Delta1, forward, CCGGCTGAAGCTACAGAAAC; Delta1, reverse, GAAAGTCCGCCTTCTTGTTG; Jagged1, forward, GGATGATGGGAACCCTGTCAAG; Jagged1, reverse, TGTTTATTTGTCCAGTTCGGGTGT; HES1, forward, CCCACCTCTCTCTTCTGACG; HES1, reverse, AGGCGCAATCCAATATGAAC; MyHCF GACCAGATCTTCCCCATGAA; MyHCR TAAGGGTTGACGGTGACACA. GAPDH, MyoD, myogenin, and Myf5 primers were as previously described (Ishibashi et al., 2005).

FACS sorting
Satellite cells were isolated as per Kuang et al. (2007). RNA was isolated from freshly sorted α7integrin$^+$, CD31$^-$/Sca1$^-$/CD45$^-$ cells, or the same cells maintained in culture for 3 d as previously described.

In situ hybridization
In situ hybridizations were performed on 8-μm cryosections of mouse tibialis anterior muscles from 2-mo-old mice according to previously described procedures (Braissant and Wahli, 1998). Sense and antisense in situ probes were synthesized from the original RDA product using DIG labeling mix (Roche) with SP6 or T7 RNA polymerase (Roche). Alkaline phosphatase–conjugated anti-DIG antibody (Roche) followed by reaction with BCIP/NBT (Roche) was used to detect hybridized cRNA probes.

Phage library screen
A commercially prepared mouse embryonic day 10.5 Lambda cDNA phage library (Stratagene) was plated at 5×10^4 plaque forming units per plate. A total of 5×10^5 plaques were plated and lifted as per the manufacturer's instructions. Plaques were screened using a radiolabeled probe generated using the original MDp67 RDA clone. Positive plaques were cored and eluted as per the manufacturer's instructions, and secondary and tertiary screens were performed at 10^3 and 10^2 plaque forming units per plate, respectively. The two positive clones were sequenced and compared/aligned using DNAStar software (DNAstar Inc.).

Retroviral production and infection
Retrovirus was generated using a modified version of the three-plasmid HIT system (provided by V. Sartorelli, National Institutes of Health, Bethesda, MD) as previously described (Soneoka et al., 1995; Ishibashi et al., 2005). For retroviral infection, C_2C_{12} cells were seeded at 10^5 cells per 10-cm plate. 8 h after plating, cells were incubated with retrovirus for 12 h with 8 μg/ml polybrene. Cells were then washed twice with PBS and maintained in growth media for 24 h before the addition of antibiotics for selection.

Protein isolation and cellular fractionation
Protein was isolated as previously described (Perry et al., 2001). For cellular fractions, cells were washed twice in ice-cold PBS-fused vesicles and scrapped off plates in 1 ml PBS-fused vesicles. Cells were pelleted, resuspended in 5 ml of ice-cold hypotonic buffer (10 mM Hepes, pH 8.0, 15 mM KCl, 2 mM $MgCl_2$, and 0.1 mM EDTA), incubated for 5 min, and lysed using a dounce homogenizer on ice. Supernatant was then centrifuged at 65,000 rpm at 4°C for 1 h using NVT100 rotor in an ultracentrifuge (Beckman Coulter). Supernatant was collected and the membrane pellet resuspended in NP-40 lysis buffer with protease inhibitors (1 mM DTT, 1 mM PMSF, 10 mg/ml pepstatin A, aprotinin, leupeptin, and 1 mM sodium vanadate). The nuclear pellet was washed once in buffer A and then incubated on ice for 20 min in buffer C. Nuclear lysates were centrifuged and supernatants were diluted with buffer D with protease inhibitors.

Western blotting
Western analysis was performed as previously described (Sabourin et al., 1999). Antibodies used for these studies were as follows: α-MyoD (C-20; Santa Cruz Biotechnology, Inc.), α-Myf5 (C-20; Santa Cruz Biotechnology, Inc.), α-Pax7 (PAX7; Developmental Studies Hybridoma Bank), α-HA (HA7; Sigma-Aldrich), α-myogenin (F5D [Developmental Studies Hybridoma Bank] or M225 [Santa Cruz Biotechnology, Inc.]), and α-MyHC (MF20; Developmental Studies Hybridoma Bank). α-Megf10 antibody was generated in rabbits against a GST fusion protein containing the carboxy-terminal 290 aa of Megf10 (Washington Biotechnology).

BrdU incorporation
C_2C_{12} myoblasts were maintained in growth media (DME supplemented with 10% FBS) or differentiation media (DME supplemented with 2% horse serum). Cells were pulsed for 30 min with 30 mM BrdU and stained using the BrdU In situ Detection kit (BD Biosciences) as per the manufacturer's instructions.

Fiber isolation and immunohistochemistry
Tibialis anterior muscles were isolated from 2-mo-old mice. Muscles were incubated overnight through a series of sucrose solutions (4, 15, and 30%). After overnight incubation in 30% sucrose/PBS, the muscles were embedded in optimal cutting temperature and flash frozen in liquid nitrogen. Sections were cut at 8 μm using a cryostat (Leica). Sections were incubated with primary antibody overnight (α-Megf10, 1:200 [Washington Biotechnology] or α–syndecan-4, 1:200 [gift from B. Olwin, University of Colorado, Boulder, CO]). FITC-conjugated α-chicken and TRITC-conjugated α-rabbit

secondaries were used for visualization. Images were obtained at room temperature using a microscope (Axioskop; Carl Zeiss, Inc.), 20× NA 0.50 plan-Neofluar (ω/0.17; Carl Zeiss, Inc.) or 40× NA 0.75 plan-Neofluar (ω/0.17; Carl Zeiss, Inc.) objective, and camera (SPOT; Diagnostic Instruments, Inc.). Images were captured using SPOT 3.5.5 software (Diagnostic Instruments, Inc.) and were processed with Photoshop (Adobe).

Fibers were isolated as previously described (Kuang et al., 2006), and either directly fixed or grown for 2–3 d in Ham's F10 media supplemented with 20% FBS, penicillin/streptomycin, and 2.5 ng/μl of basic FGF (Ham's complete) on horse serum–coated culture dishes. Individual fibers were fixed, permeabilized, and incubated with primary antibodies at the following dilutions: α-Megf10, 1:50; α-Pax7, 1:10; α–M-cadherin, 1:200; α–syndecan-4, 1:200; α-MyoD, 1:50; α–myogenin F5D, 1:10; and α-myogenin M225,1:50. Secondary antibodies used were Alexa 488, Alexa 568, and Alexa 647 conjugated to specific IgG types (Invitrogen) that matched the primary antibodies.

Images were obtained using a microscope (Axioplan2; Carl Zeiss, Inc.), a 20× NA 0.75 plan Apochromat (ω/0.17; Carl Zeiss, Inc.) objective, and a digital camera (Axiocam; Carl Zeiss, Inc.). Digital images were captured using Axiovision (Carl Zeiss, Inc.) and were processed with Photoshop.

Megf10 siRNA and shRNA knockdown

EDL fibers were plated in media without antibiotics, and transfection was carried at 24 h after dissection using Lipofectamine 2000 reagent (Invitrogen) as per the manufacturer's instructions. Three different siRNA duplexes were used at the final concentration of 20 nM each. Fibers were refed in fresh media with antibiotics on the next morning and fixed after 60–72 h of culture.

MyoD$^{-/-}$ primary myoblasts were grown on 10-cm collagen-coated dishes in Ham's F10 media supplemented with 20% FBS, penicillin/streptomycin, and 2.5 ng/μl of basic FGF (Ham's Complete). Cells were refed 3 h before transfection with serum-free media and transfected with a mix of three different shRNA plasmids (OpenBiosystems) for a total of 4 μg of plasmid DNA, using ArrestIn transfection reagent (OpenBiosystems) as per the manufacturer's instructions. Cells were washed and re-fed with Ham's complete media 6 h after transfections. RNA was harvested 48 h after transfection.

We thank Dr. V. Sartorelli for providing retroviral expression plasmids and Mark Gillespie and Dr. Iain McKinnell for careful reading of the manuscript.

M.A. Rudnicki holds the Canada Research Chair (CRC) in Molecular Genetics and is an International Research Scholar of the Howard Hughes Medical Institute (HHMI). This work was supported by grants to M.A. Rudnicki from the Muscular Dystrophy Association, the National Institutes of Health (R01AR044031), the Canadian Institutes of Health Research (MOP12080), the HHMI, and the CRC Program.

Submitted: 13 September 2007
Accepted: 31 October 2007

References

Anderson, J.E. 2000. A role for nitric oxide in muscle repair: nitric oxide-mediated activation of muscle satellite cells. *Mol. Biol. Cell*. 11:1859–1874.

Beauchamp, J.R., L. Heslop, D.S. Yu, S. Tajbakhsh, R.G. Kelly, A. Wernig, M.E. Buckingham, T.A. Partridge, and P.S. Zammit. 2000. Expression of CD34 and Myf5 defines the majority of quiescent adult skeletal muscle satellite cells. *J. Cell Biol.* 151:1221–1234.

Bischoff, R. 1994. The satellite cell and muscle regeneration. *In* Myogenesis. A.G. Engel and C. Franszini-Armstrong, editors. McGraw-Hill, New York. 97–118.

Braissant, O., and W. Wahli. 1998. Differential expression of peroxisome proliferator-activated receptor-alpha, -beta, and -gamma during rat embryonic development. *Endocrinology*. 139:2748–2754.

Charge, S.B., and M.A. Rudnicki. 2004. Cellular and molecular regulation of muscle regeneration. *Physiol. Rev.* 84:209–238.

Clegg, C.H., T.A. Linkhart, B.B. Olwin, and S.D. Hauschka. 1987. Growth factor control of skeletal muscle differentiation: commitment to terminal differentiation occurs in G_1 phase and is repressed by fibroblast growth factor. *J. Cell Biol.* 105:949–956.

Collins, C.A., I. Olsen, P.S. Zammit, L. Heslop, A. Petrie, T.A. Partridge, and J.E. Morgan. 2005. Stem cell function, self-renewal, and behavioral heterogeneity of cells from the adult muscle satellite cell niche. *Cell*. 122:289–301.

Conboy, I.M., and T.A. Rando. 2002. The regulation of Notch signaling controls satellite cell activation and cell fate determination in postnatal myogenesis. *Dev. Cell*. 3:397–409.

Conboy, I.M., M.J. Conboy, G.M. Smythe, and T.A. Rando. 2003. Notch-mediated restoration of regenerative potential to aged muscle. *Science*. 302:1575–1577.

Conboy, I.M., M.J. Conboy, A.J. Wagers, E.R. Girma, I.L. Weissman, and T.A. Rando. 2005. Rejuvenation of aged progenitor cells by exposure to a young systemic environment. *Nature*. 433:760–764.

Cornelison, D.D., and B.J. Wold. 1997. Single-cell analysis of regulatory gene expression in quiescent and activated mouse skeletal muscle satellite cells. *Dev. Biol.* 191:270–283.

Cornelison, D.D., M.S. Filla, H.M. Stanley, A.C. Rapraeger, and B.B. Olwin. 2001. Syndecan-3 and syndecan-4 specifically mark skeletal muscle satellite cells and are implicated in satellite cell maintenance and muscle regeneration. *Dev. Biol.* 239:79–94.

Freeman, M.R., J. Delrow, J. Kim, E. Johnson, and C.Q. Doe. 2003. Unwrapping glial biology: Gcm target genes regulating glial development, diversification, and function. *Neuron*. 38:567–580.

Hamon, Y., D. Trompier, Z. Ma, V. Venegas, M. Pophillat, V. Mignotte, Z. Zhou, and G. Chimini. 2006. Cooperation between engulfment receptors: the case of ABCA1 and MEGF10. *PLoS ONE*. 1:e120.

Holterman, C.E., and M.A. Rudnicki. 2005. Molecular regulation of satellite cell function. *Semin. Cell Dev. Biol.* 16:575–584.

Ishibashi, J., R.L. Perry, A. Asakura, and M.A. Rudnicki. 2005. MyoD induces myogenic differentiation through cooperation of its NH_2- and COOH-terminal regions. *J. Cell Biol.* 171:471–482.

Jennische, E., S. Ekberg, and G.L. Matejka. 1993. Expression of hepatocyte growth factor in growing and regenerating rat skeletal muscle. *Am. J. Physiol.* 265:C122–C128.

Krivtsov, A.V., F.N. Rozov, M.V. Zinovyeva, P.J. Hendrikx, Y. Jiang, J.W. Visser, and A.V. Belyavsky. 2007. Jedi—a novel transmembrane protein expressed in early hematopoietic cells. *J. Cell. Biochem.* 101:767–784.

Kuang, S., S.B. Charge, P. Seale, M. Huh, and M.A. Rudnicki. 2006. Distinct roles for Pax7 and Pax3 in adult regenerative myogenesis. *J. Cell Biol.* 172:103–113.

Kuang, S., K. Kuroda, F. Le Grand, and M.A. Rudnicki. 2007. Asymmetric self-renewal and commitment of satellite stem cells in muscle. *Cell*. 129:999–1010.

Mauro, A. 1961. Satellite cell of skeletal muscle fibers. *J. Biophys. Biochem. Cytol.* 9:493–495.

Megeney, L.A., B. Kablar, K. Garrett, J.E. Anderson, and M.A. Rudnicki. 1996. MyoD is required for myogenic stem cell function in adult skeletal muscle. *Genes Dev.* 10:1173–1183.

Nagase, T., M. Nakayama, D. Nakajima, R. Kikuno, and O. Ohara. 2001. Prediction of the coding sequences of unidentified human genes. XX. The complete sequences of 100 new cDNA clones from brain which code for large proteins in vitro. *DNA Res.* 8:85–95.

Nofziger, D., A. Miyamoto, K.M. Lyons, and G. Weinmaster. 1999. Notch signaling imposes two distinct blocks in the differentiation of C2C12 myoblasts. *Development*. 126:1689–1702.

Perry, R.L., M.H. Parker, and M.A. Rudnicki. 2001. Activated MEK1 binds the nuclear MyoD transcriptional complex to repress transactivation. *Mol. Cell*. 8:291–301.

Sabourin, L.A., A. Girgis-Gabardo, P. Seale, A. Asakura, and M.A. Rudnicki. 1999. Reduced differentiation potential of primary *MyoD −/−* myogenic cells derived from adult skeletal muscle. *J. Cell Biol.* 144:631–643.

Schultz, E. 1996. Satellite cell proliferative compartments in growing skeletal muscles. *Dev. Biol.* 175:84–94.

Seale, P., J. Ishibashi, C. Holterman, and M.A. Rudnicki. 2004. Muscle satellite cell-specific genes identified by genetic profiling of MyoD-deficient myogenic cell. *Dev. Biol.* 275:287–300.

Soneoka, Y., P.M. Cannon, E.E. Ramsdale, J.C. Griffiths, G. Romano, S.M. Kingsman, and A.J. Kingsman. 1995. A transient three-plasmid expression system for the production of high titer retroviral vectors. *Nucleic Acids Res.* 23:628–633.

Sun, H., L. Li, C. Vercherat, N.T. Gulbagci, S. Acharjee, J. Li, T.K. Chung, T.H. Thin, and R. Taneja. 2007. Stra13 regulates satellite cell activation by antagonizing Notch signaling. *J. Cell Biol.* 177:647–657.

Suzuki, E., and M. Nakayama. 2007. The mammalian Ced-1 ortholog MEGF10/KIAA1780 displays a novel adhesion pattern. *Exp. Cell Res.* 313:2451–2464.

Tatsumi, R., J.E. Anderson, C.J. Nevoret, O. Halevy, and R.E. Allen. 1998. HGF/SF is present in normal adult skeletal muscle and is capable of activating satellite cells. *Dev. Biol.* 194:114–128.

Tatsumi, R., S.M. Sheehan, H. Iwasaki, A. Hattori, and R.E. Allen. 2001. Mechanical stretch induces activation of skeletal muscle satellite cells in vitro. *Exp. Cell Res.* 267:107–114.

Tatsumi, R., A. Hattori, Y. Ikeuchi, J.E. Anderson, and R.E. Allen. 2002. Release of hepatocyte growth factor from mechanically stretched skeletal

muscle satellite cells and role of pH and nitric oxide. *Mol. Biol. Cell*. 13:2909–2918.

Tatsumi, R., X. Liu, A. Pulido, M. Morales, T. Sakata, S. Dial, A. Hattori, Y. Ikeuchi, and R.E. Allen. 2006. Satellite cell activation in stretched skeletal muscle and the role of nitric oxide and hepatocyte growth factor. *Am. J. Physiol. Cell Physiol.* 290:C1487–C1494.

Ustanina, S., J. Carvajal, P. Rigby, and T. Braun. 2007. The myogenic factor myf5 supports efficient skeletal muscle regeneration by enabling transient myoblast amplification. *Stem Cells*. 25:2006–2016.

Vasyutina, E., D.C. Lenhard, H. Wende, B. Erdmann, J.A. Epstein, and C. Birchmeier. 2007. RBP-J (Rbpsuh) is essential to maintain muscle progenitor cells and to generate satellite cells. *Proc. Natl. Acad. Sci. USA*. 104:4443–4448.

Wozniak, A.C., and J.E. Anderson. 2007. Nitric oxide-dependence of satellite stem cell activation and quiescence on normal skeletal muscle fibers. *Dev. Dyn.* 236:240–250.

Yoshida, N., S. Yoshida, K. Koishi, K. Masuda, and Y. Nabeshima. 1998. Cell heterogeneity upon myogenic differentiation: down-regulation of MyoD and Myf-5 generates 'reserve cells'. *J. Cell Sci.* 111:769–779.

Zammit, P.S., J.P. Golding, Y. Nagata, V. Hudon, T.A. Partridge, and J.R. Beauchamp. 2004. Muscle satellite cells adopt divergent fates: a mechanism for self-renewal? *J. Cell Biol.* 166:347–357.

Zhou, Z., E. Hartwieg, and H.R. Horvitz. 2001. CED-1 is a transmembrane receptor that mediates cell corpse engulfment in *C. elegans*. *Cell*. 104:43–56.